From Tortoise-Shell-Like Molecular Segments to $C_{4n}H_{2n}N_{2n}$ ($n = 3-8$) Cages Stabilized by Alkenyl: A Theoretical Study

Liang-Wei Shi,[†] Wen-Ming Wu,[‡] Gang Zhao,*[,†] and Min-Bo Chen*[,†]

Shanghai Institute of Organic Chemistry, Chinese Academy of Sciences, 354 Fenglin Road, Shanghai 200032, China, and Xi'an Institute of High Technology and Science, Xi'an, 710025, China

Received: December 14, 2009; Revised Manuscript Received: January 28, 2010

The $C_{4n}H_{2n}N_{2n}$ ($n = 3-8$) cage molecules with D_{nh} symmetry and their nitrated products, $C_{4n}N_{4n}O_{4n}$ ($n = 3$, 4, 5) and $C_{4n}H_nN_{3n}O_{2n}$ ($n = 4$, 6, 8) were studied by DFT at the B3LYP/cc-pVDZ level. Their geometrical structures, ground-state energies, and heats of formation have been investigated. They exhibit an obvious cage effect. Hirshfeld partitioning charges in momentum space give evidence of high strained energy in the title compounds. Their orbital energy and frontier orbital shape and electrostatic potential calculation are also studied. Investigation of heat of formation and NICS analysis reveal that $C_{24}H_{12}N_{12}$ is the most stable molecule among title compounds with D_{nh} symmetry. Their half nitrated products are predicted as a promising candidate for high energy matter.

1. Introduction

In nonmetallic elements, C, B, and N are the most common atoms that can make up cage-like molecules. They are characteristic of classical molecular strain and special bonding so that they possess special properties. It stimulates the curiosity of chemists and physists continually. Fullerenes are representative of the cages consisting of carbon atoms.[1−3] When these molecules are hydrogenated, some polyhedral hydrocarbons can be easily formed. These cages range from some small cages, e.g., cubane, tetrahedrane, dodecahedrane,[4] etc., to medium-sized hydrocarbons.[5] As for those molecules consisting of boron atoms, borane and carborane are familiar to us.[6] At present, those cage-like molecules with pure nitrogen and polymeric nitrogen are still on the stage of theoretical investigation. Usually, to enhance the certain properties of these cage-like molecules, chemists dope them with different atoms. For example, carbon atoms in fullerenes are substituted by boron or nitrogen atoms,[7] those in hydrocarbons cages by nitrogen atoms,[8] and nitrogen atoms in N_n cages by sulfur atom[9] or by oxygen atoms.[10,11] In fact, high symmetric cages consisted of carbon and nitrogen atoms have been a focus of our attention recently.[12] In these systems, groups such as >N—N< and >C═C< play a key role in stabilizing these molecules.

Our interests come from two aspects, one is the scientific exploration for aesthetically pleasing structures, and the other is to find potential application in new materials. During the process of the design of new cage-like molecules consisting of carbon and nitrogen atoms, we have theoretically designed $C_{4n}N_{2n}$ ($n = 3-8$) and their hydrogenated products $C_{4n}H_{4n}N_{2n}$ ($n = 3-8$).[12] $C_{32}N_{16}$ with D_{8h} symmetry shows higher relative stability and a potential application in high energy density matter. In these molecules, >N—*N*< stabilizes the cage backbones. When carbon and nitrogen atoms in the middle of these cages alternate, a new analogy of $C_{4n}N_{2n}$ ($n = 3-8$) connected by >C═C< groups can be found. If they are further saturated by hydrogen only for those carbons in top and bottom polygons, a new series of $C_{4n}H_{2n}N_{2n}$ ($n = 3-8$) cages in D_{nh} ($n = 3-8$) symmetry will be formed, as shown in Figure 1. During the investigation, some analogies of our title compounds, such as sunflower-like carbon−sulfur molecules,[13] cylindrical N_{18} and phosphorus substitution $N_{12}P_6$ are found.[14] To our knowledge, these designed title molecules have not been reported yet except a study of an analogy of $C_{24}H_{12}N_{12}$ molecule.[7] To compare relative stability and potential energetic property of nitrated products of $C_{4n}H_{2n}N_{2n}$ ($n = 3-8$) cages, six cage molecules, $C_{4n}N_{4n}O_{4n}$ ($n = 3$, 4, 5) and $C_{4n}H_nN_{3n}O_{2n}$ ($n = 4$, 6, 8), are designed additionally. They are divided into two groups. The former is fully substituted on hydrogen atoms by NO_2 groups ($C_{12}N_{12}O_{12}$, $C_{16}N_{16}O_{16}$, $C_{20}N_{20}O_{20}$ in Figure 2), and the later belongs to those with half substitution ($C_{16}H_4N_{12}O_8$, $C_{24}H_6N_{18}O_{12}$, $C_{32}H_8N_{24}O_{16}$ in Figure 2).

It must be clarified that our design should be based on those candidate compounds obtainable in regular organic synthesis. So, our designed polynitrogen cages should have proper size and suitable bonding groups. Systematically theoretical studies for the designed species including molecular structures, orbital properties, thermochemical properties, and electrostatic and aromatic characters are necessary. This study will provide heuristic information for experimental work. If these molecules will be synthesized, they have superior high energy properties, or polymerization ability like POSS cages.[15]

2. Computational Details

Full geometric optimization at ground-state and vibrational frequencies calculation were performed with the B3LYP/cc-pVDZ model. The cc-pVDZ basis set belongs to one of Dunning's correlation consistent basis sets,[16] which include valence polarization functions with 2s, 1p on H and 3s, 2p, 1d on C, N, and O and behave higher computational efficiency. The optimization of $C_{4n}H_{2n}N_{2n}$ ($n = 3-8$) cage molecules was successfully performed in D_{nh} ($n = 3-8$) symmetry. Although those molecules with NO_2 groups have less symmetry, our optimization for $C_{4n}N_{4n}O_{4n}$ ($n = 3$, 4, 5) and $C_{4n}H_nN_{3n}O_{2n}$ ($n = 4$, 6, 8) nitrated cages is still performed with higher symmetry at the first step. When imaginary vibrational frequency appears, the lower symmetry of struc-

[†] Chinese Academy of Sciences.
[‡] Xi'an Institute of High Technology and Science.

10.1021/jp911788p
Published on Web 02/15/2010

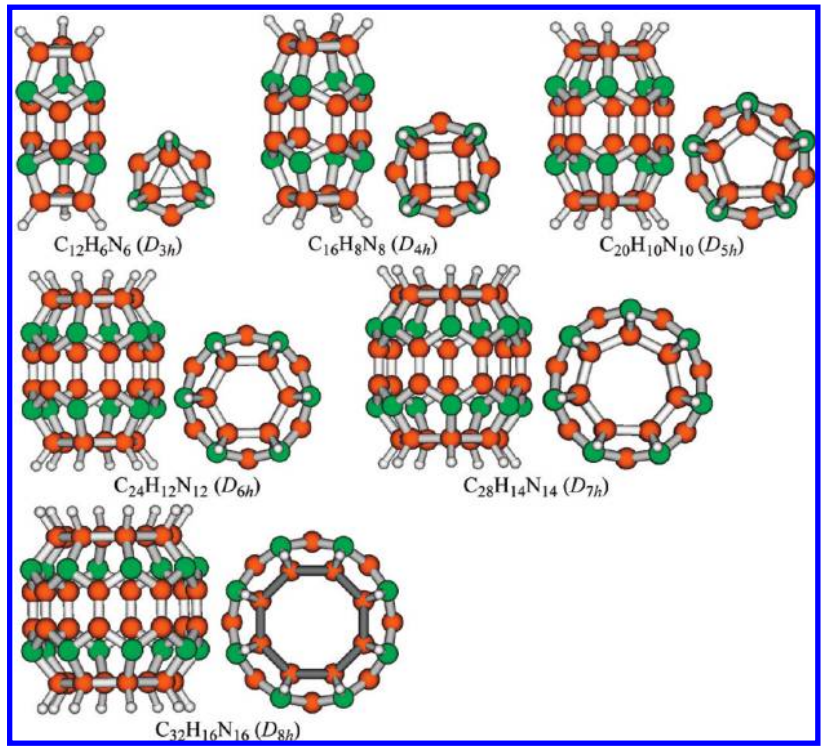

Figure 1. Optimized structures of $C_{4n}H_{2n}N_{2n}$ ($n = 3-8$) cages in D_{nh} symmetry (side view in left and top view in right). Green stands for nitrogen atoms, and the orange for carbon.

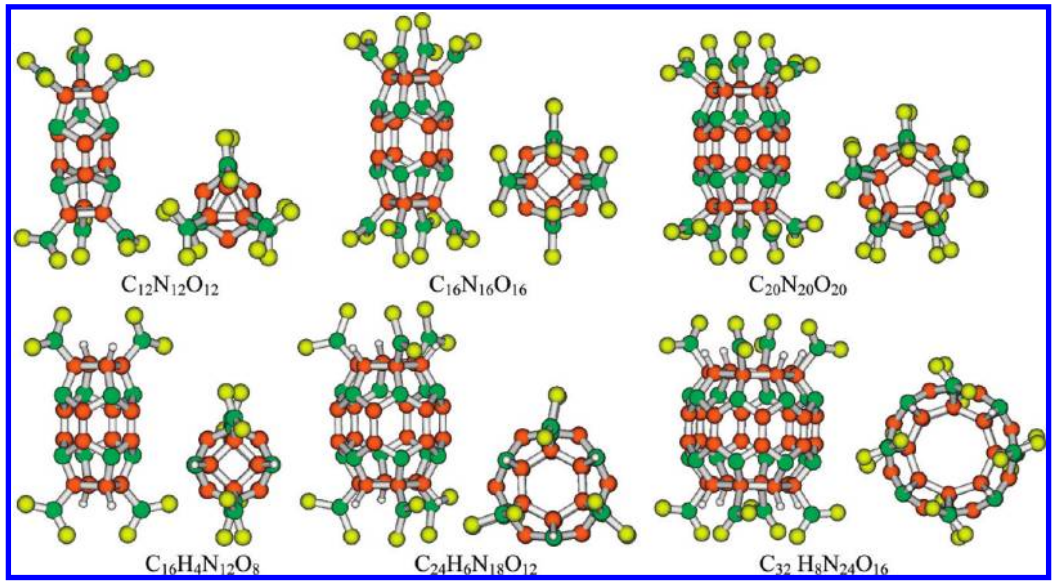

Figure 2. Optimized structures of $C_{4n}N_{4n}O_{4n}$ ($n = 3-5$) and $C_{4n}H_nN_{3n}O_{2n}$ ($n = 4, 6, 8$) cages (side view in left and top view in right). Green stands for nitrogen atoms, orange for carbon, and yellow for oxygen.

tures and structure adjustment by the atomic amplitude of the highest/high imaginary frequency is always employed to obtain successful optimization. The calculations of the harmonic vibrational frequencies for the optimized equilibrium geometries show that they correspond to minima on the hypersurface of potential energy. After the equilibrium geometries are established, the electronic stability and orbital energy are investigated. Usually, the vertical ionization potential and the electron affinity can be obtained by Koopman's theorem, which relates them to the negative orbital energies.

The extent of electron delocalization is usually revealed by nucleus-independent chemical shifts (NICS) in Schleyer's paper,[17] which equals the negative of the isotropic nuclear magnetic shielding tensor of the ghost atom. It has also been used to indicate the aromaticity for some polyhedral hydrocarbon and doped fullerenes.[12] The gauge-independent atomic orbital (GIAO) method[18] is used in the calculation of NICS at the B3LYP/cc-pVDZ level. The GIAO procedure is designed so that the magnetic properties of the atoms are invariant to the choice of coordinate axis. For the calculation of electrostatic potential (ESP), the fine grid was taken to generate ESP points. All of the calculations depicted above were performed in Gaussian 03 program.

After the geometric optimization was performed with the basis set of B3LYP/cc-pVDZ by Gaussian 03 program, the Hirshfeld charges of the molecules were then obtained by BLYP/DNP and PW91/DNP single point computations using DMol[3] software.

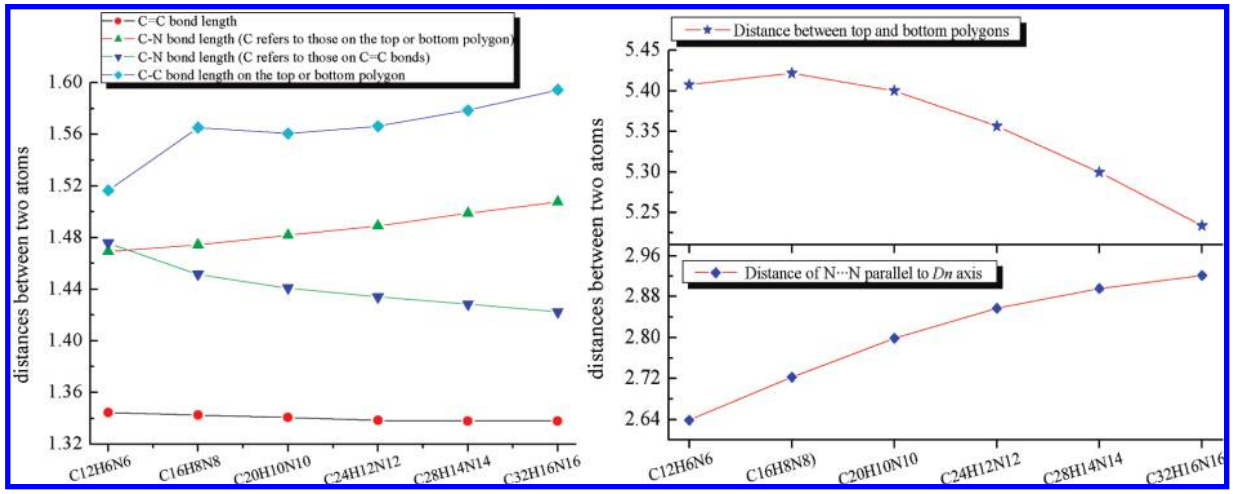

Figure 3. Main distances between two atoms in $C_{4n}H_{2n}N_{2n}$ ($n = 3-8$) molecules.

3. Results and Discussion

3.1. Structural Character. The initial optimizations for $C_{4n}H_{2n}N_{2n}$ ($n = 3-8$) cage molecules were successful in D_{nh} ($n = 3-8$) symmetry. These optimized structures are depicted with side view and top view in Figure 1. All the structures in Figure 1 are composed of $2n$ ($n = 3-8$) five-membered rings and n ($n = 3-8$) six-membered rings except the top and bottom polygons. The optimizations for nitrated products of $C_{4n}H_{2n}N_{2n}$ ($n = 3-8$) cages were also successful and are depicted in Figure 2. The selected geometric parameters (in Å for bond lengths and degree for angles) of all title species are provided in the Supporting Information S1.

In our title compounds, there are six characteristic bonds, i.e., the distance of N···N parallel to the D_n axis ($d_{N\cdots N}$), C═C bond length ($d_{C=C}$), C—C bond length in the top and bottom polygons (d_{C-C}), C—N bond length where C is in the top and bottom polygons (d_{C-N}), C—N bond length where C is in C═C (d'_{C-N}), and the distance between the top and bottom polygons (d_{plane}). The $d_{N\cdots N}$ is also used to denote the corresponding distances between two N atoms in $C_{4n}N_{4n}O_{4n}$ ($n = 3, 4, 5$) and $C_{4n}H_nN_{3n}O_{2n}$ ($n = 4, 6, 8$) cages unless noted elsewhere, although symmetry is getting lower in them.

Figure 3 shows the changes of geometrical parameters in $C_{4n}H_{2n}N_{2n}$ ($n = 3-8$) series. $d_{C=C}$ exhibits a slightly decrease from $n = 3$ to 8, but they are all a little bit longer than that in ethylene, 1.333 Å. It is possibly due to the caging effect. The cage effect is more or less an obscure concept. However, for $C_{4n}H_{2n}N_{2n}$ ($n = 3-8$) title molecules in Figure 2, it is evident from Figure 3 that the d_{plane} decreases monotonically with the order 5.422, 5.400, 5.356, 5.300, and 5.234 Å for n from 4 to 8, and the d_{plane} in $C_{12}H_6N_6$ shows a little deviation. In brief, a bigger cage size causes a more spherical shape. The whole series have n ($n = 3-8$) pyrazine rings without hydrogen atoms. The $d_{N\cdots N}$ increases linearly from the smallest cage to the largest cage. So the pyrazine rings tend to be planar. Moreover, d_{C-N} shows an increase tendency for n from 3 to 8, while d'_{C-N} shows an inverse in Figure 3.

d_{C-C} in $C_{4n}H_{2n}N_{2n}$ ($n = 3-8$) cages become longer in comparison with that in $C_{4n}N_{2n}$ ($n = 3-8$) but are similar to that in $C_{4n}H_{4n}N_{2n}$ ($n = 3-8$).[12] It is attributed to the fact that the bond energy is released when saturated by hydrogen so that bond lengths become longer. The C—C bond lengths in the top and bottom polygons are 1.517 Å in $C_{12}H_6N_6$, 1.565 Å in $C_{16}H_8N_8$, 1.561 Å in $C_{20}H_{10}N_{10}$, 1.566 Å in $C_{24}H_{12}N_{12}$, 1.579 Å in $C_{28}H_{14}N_{14}$, and 1.595 Å in $C_{32}H_{16}N_{16}$. The corresponding average C—C bond lengths in cycloalkanes, C_nH_{2n} ($n = 3-8$), calculated at the B3LYP/cc-pVDZ level, are 1.510, 1.554, 1.546, 1.536, 1.539, and 1.540 Å. It is found that the top or bottom polygon in $C_{4n}H_{2n}N_{2n}$ ($n = 3-8$) is kept planar, and the planar structure is also kept in cyclopropane, but not in cycloalkanes, C_nH_{2n} ($n = 4-8$). Therefore, only the calculated d_{C-C} in $C_{12}H_6N_6$ is consistent with that in cyclopropane basically, and there exists no such consistency of calculated d_{C-C} between that in $C_{4n}H_{2n}N_{2n}$ ($n = 4-8$) and the corresponding one in cycloalkanes, C_nH_{2n} ($n = 4-8$). As for the abnormal short d_{C-C} (1.517 Å) on the top or bottom polygon in $C_{12}H_6N_6$ in comparison with those (1.565−1.595 Å) of other $C_{4n}H_{2n}N_{2n}$ ($n = 4-8$) compounds, it is justified by the strong σ aromatic character in the triangle to be revealed by the calculation of NICS in a later section.

As mentioned above, those cycloalkanes, C_nH_{2n} ($n = 3-8$), form plane polygons when they are embedded in the title cage molecules. Intuitively, it is considered that there is more or less strained energy. Qualitative judgment can be performed by recent momentum density research of strained system/unstrained reference by Balanarayan.[19] Synoptically, the momentum density is taken as an indicator of molecular strain, and its criterion can be brought out by Hirshfeld partitioning in momentum space. We calculated Hirshfeld charges of those carbon and hydrogen atoms on the top and bottom polygons and those in corresponding cycloalkanes, C_nH_{2n} ($n = 3-8$), for comparison (data in the Supporting Information). Analyzing the calculated results for title molecules reveals that the carbon atoms become less negative and the hydrogen atoms are more positive in comparison with the unstrained or less strained cycloalkanes whatever BLYP/DNP or PW91/DNP level was used. The depletion of charge density of the bonding region in single cycloalkanes, C_nH_{2n} ($n = 3-8$), results in a buildup of charge density of the top and bottom polygons in title cage molecules.[19] It indicates that these cage molecules accumulate more strain energy when they are made up by less-strained molecular segments.

For $C_{4n}N_{4n}O_{4n}$ ($n = 3, 4, 5$) series, $d_{N\cdots N}$, $d_{C=C}$, and d_{plane} show a decreased tendency with respect to their precursors. For $C_{4n}H_nN_{3n}O_{2n}$ ($n = 4, 6, 8$) series, $d_{C=C}$ becomes shorter or the C═C bonds become strong, and a longer $d_{N\cdots N}$ was found in the longitudinal distance of H—C—N···N—C—H, while a shorter $d_{N\cdots N}$ in the distance of O_2N—C—N···N—C—NO_2. Then a corresponding change was also found in d_{plane}. It is interesting that the average d_{C-C} becomes longer in $C_{4n}N_{4n}O_{4n}$ ($n = 3, 4,$

TABLE 1: Ground-State Energies ε_0 (au), $\Delta H°_f$ (kcal/mol), Group ε_0 (au), and Group $\Delta H°_{f,298K}$ (kcal/mol)

formula	ε_0	$\Delta H°_f$	group ε_0	group $\Delta H°_f$
$C_{12}H_6N_6$ (D_{3h})	−788.99696	414.69	−262.99899	138.23
$C_{16}H_8N_8$ (D_{4h})	−1052.23708	405.68	−263.05927	101.42
$C_{20}H_{10}N_{10}$ (D_{5h})	−1315.44658	415.42	−263.08932	83.08
$C_{24}H_{12}N_{12}$ (D_{6h})	−1578.54266	495.86	−263.09044	82.64
$C_{28}H_{14}N_{14}$ (D_{7h})	−1841.57326	616.72	−263.08189	88.10
$C_{32}H_{16}N_{16}$ (D_{8h})	−2104.56640	761.13	−263.07080	95.14
$C_{12}N_{12}O_{12}$	−2015.97036	757.45	−671.99012	252.48
$C_{16}N_{16}O_{16}$	−2688.24872	836.12	−672.06218	209.03
$C_{20}N_{20}O_{20}$	−3360.41351	981.04	−672.08270	196.21
$C_{16}H_4N_{12}O_8$	−1870.27994	598.23	−467.56999	149.56
$C_{24}H_6N_{18}O_{12}$	−2805.61080	780.53	−467.60180	130.09
$C_{32}H_8N_{24}O_{16}$	−3740.63799	1152.01	−467.57975	144.00

5), and shorter in $C_{4n}H_nN_{3n}O_{2n}$ (n = 4, 6, 8) with respect to their precursors without nitration. Apparently, more nitration causes more repulsive force to decrease their stability.

3.2. Thermochemical Properties. A systematic study on chemical stability for title compounds, $C_{4n}H_{2n}N_{2n}$ (n = 3−8), $C_{4n}N_{4n}O_{4n}$ (n = 3, 4, 5), and $C_{4n}H_nN_{3n}O_{2n}$ (n = 4, 6, 8), at the ground state is conducted by thermochemical calculation. The isodesmic reaction approach is normally taken for the calculation of the gas-phase heat of formation ($\Delta H°_f$). The designed isodesmic reactions are presented as follows:

$$C_{4n}H_{2n}N_{2n}\ (n = 3-8) + 8nCH_4 \rightarrow 2nN(CH_3)_3 + nH_2C{=}CH_2 + 2nCH_3CH_3 \quad (1)$$

$$C_{4n}N_{4n}O_{4n}\ (n = 3-5) + 8nCH_4 \rightarrow 2nN(CH_3)_3 + nH_2C{=}CH_2 + 2nCH_3CH_2NO_2 \quad (2)$$

$$C_{4n}H_nN_{3n}O_{2n}\ (n = 4, 6, 8) + 8nCH_4 \rightarrow 2nN(CH_3)_3 + nH_2C{=}CH_2 + nCH_3CH_2NO_2 + nCH_3CH_3 \quad (3)$$

To obtain the change of reaction enthalpy ΔH of isodesmic reactions in eqs 1−3, theoretical electronic energies at the B3LYP/cc-pVDZ level and thermal enthalpies from statistical thermodynamic calculation are always first performed for all title molecules, CH_4, $N(CH_3)_3$, C_2H_4, $CH_3CH_2NO_2$, and C_2H_6. The calculated data are listed in the Supporting Information in which the sum of electronic and thermal enthalpies has included zero point correction. It is known that the experimental $\Delta H°_f$ of trimethylamine, ethylene, ethane, methane, and nitroethane are −23.70, 52.47, −83.80, −74.50, and −102.40 kJ·mol^{-1}, respectively. Their references and the detailed isodesmic reaction equations are all provided in Supporting Information S4. Then the calculated standard $\Delta H°_f$ of title compounds tabulated in Table 1 can be easily obtained.

The group energies and heat of formation (group $\Delta H°_f$)[12] for $C_{4n}H_{2n}N_{2n}$ (n = 3−8), $C_{4n}N_{4n}O_{4n}$ (n = 3, 4, 5), and $C_{4n}H_nN_{3n}O_{2n}$ (n = 4, 6, 8) species were obtained from the calculated results of their total ground-state energies and $\Delta H°_f$ divided by n. The results are listed in Table 1. The group $\Delta H°_f$ can be regarded as the average enthalpy increment in the process of adding one more group of >CH−N−C=C−N−CH< . In searching of high energy density molecules, people want to have a compound with high heat of formation at the expense of chemical stability as low as possible. Therefore, lower group $\Delta H°_f$ is preferable for searching high energy density molecules. It is the sense of "relative chemical stability" cited hereafter. In $C_{4n}H_{2n}N_{2n}$ (n = 3−8) species, a descending order for group energies and group $\Delta H°_f$, $n = 3 > 4 > 8 > 7 > 5 \approx 6$, is found. So the order of the relative chemical stability of $C_{4n}H_{2n}N_{2n}$ (n = 3−8) is $n = 6 \approx 5 > 7 > 8 > 4 > 3$. It indicates that $C_{20}H_{10}N_{10}$ and $C_{24}H_{12}N_{12}$ are the highest relative chemically stable molecules among $C_{4n}H_{2n}N_{2n}$ (n = 3−8) species at the B3LYP/cc-pVDZ level. The >C=C< groups stabilize such moderate sized cages. In nitration cage species, there are two descending orders of group energies and group $\Delta H°_f$, $C_{12}N_{12}O_{12} > C_{16}N_{16}O_{16} > C_{20}N_{20}O_{20}$ for $C_{4n}N_{4n}O_{4n}$ (n = 3, 4, 5) and $C_{16}H_4N_{12}O_8 > C_{32}H_8N_{24}O_{16} > C_{24}H_6N_{18}O_{12}$ for $C_{4n}H_nN_{3n}O_{2n}$ (n = 4, 6, 8). According to the principle of the lowest group energies and group $\Delta H°_f$ for the highest relative stable structure, $C_{20}N_{20}O_{20}$ in $C_{4n}N_{4n}O_{4n}$ species with n = 5 and $C_{24}H_6N_{18}O_{12}$ in $C_{4n}H_nN_{3n}O_{2n}$ species with n = 6 are the highest relative stable compounds after nitration.

In addition, it is noted that the lowest reaction enthalpy of the reverse reaction of eqs 1−3 (see the Support Information) correspond to those molecules with n = 6 in title species. Although the $C_{24}N_{24}O_{24}$ in $C_{4n}N_{4n}O_{4n}$ species with n = 6 is not included, it could also be a chemically and thermochemically stable one in $C_{4n}N_{4n}O_{4n}$ (n = 3−8) species. So we should pay more attention to the precursor $C_{24}H_{12}N_{12}$ and its nitrated products. Of course, it should be pointed out that the molecular stability discussed above is only a relative comparison among $C_{4n}H_{2n}N_{2n}$ (n = 3−8) series in D_{nh} (n = 3−8) symmetry. There might be some isomers for each optimized cage structure, in which the optimized cage structure may not be the most stable structure among the isomers. Theoretical comparison between those isomers also deserves further investigation.

It is evident that the nitration of model compounds increases the heat of formation, i.e., the energetic performance. The increment of heat of formation due to each addition of nitro group for $C_{4n}N_{4n}O_{4n}$ (n = 3, 4, 5) is 55−60 kcal/mol with respect to their precursor in $C_{4n}H_{2n}N_{2n}$ (n = 3, 4, 5), and that for $C_{4n}H_nN_{3n}O_{2n}$ (n = 4, 6, 8) is 49−50 kcal/mol with respect to their precursor in $C_{4n}H_{2n}N_{2n}$ (n = 4, 6, 8). As those of nitrated cages exhibit high energetic performance, they need further experimental study, and the same is true for $C_{4n}H_{2n}N_{2n}$ (n = 3−8), particularly for $C_{24}H_{12}N_{12}$. We split the $C_{24}H_{12}N_{12}$ into several segments with the shape of a tortoise shell. They can be merged into $C_{24}H_{12}N_{12}$ conceptually and experimentally through skillful synthetic technique. The sketch map of tortoise-shell-like molecular segments and the proposed reaction with two segments is shown in Figure 4. The molecular segments and the $C_{24}H_{12}N_{12}$ molecule will be studied in our laboratory experimentally. The orbital properties, aromaticity, and electrostatic potential of $C_{24}H_{12}N_{12}$ and others in the $C_{4n}H_{2n}N_{2n}$ (n = 3−8) series will also be studied in the next section.

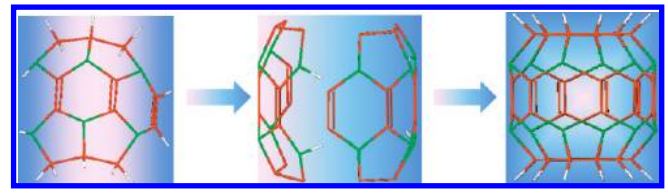

Figure 4. Sketch map of tortoise-shell-like molecular segment and corresponding reaction of two segments. Green stands for nitrogen atom, and the orange for carbon.

3.3. Orbital Properties. It is helpful to examine the electronic stability of $C_{4n}H_{2n}N_{2n}$ (n = 3−8) species through exploring their orbital energy. The calculated ionization potential, electron affinity, and orbital gap (LUMO−HOMO) values are 5.53, 3.70, and 1.84 eV for $C_{12}H_6N_6$, 4.48, 2.14, and 2.74 eV for $C_{16}H_8N_8$, 4.45, 0.88, and 3.57 eV for $C_{20}H_{10}N_{10}$, 4.27, 0.01, and 4.27 eV for $C_{24}H_{12}N_{12}$, 4.23, −0.08, and 4.30 eV for

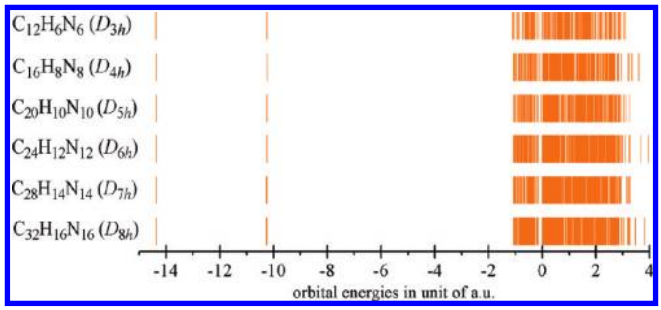

Figure 5. Orbital energy spectrum of $C_{4n}H_{2n}N_{2n}$ ($n = 3-8$) molecules.

$C_{28}H_{14}N_{14}$, and 4.25, 0.03, and 4.22 eV for $C_{32}H_{16}N_{16}$. The orbital energy spectrum of $C_{4n}H_{2n}N_{2n}$ ($n = 3-8$) molecules were plotted in Figure 5. An increasing orbital gap from $n = 3$ to 8 in $C_{4n}H_{2n}N_{2n}$ ($n = 3-8$) is found. $C_{24}H_{12}N_{12}$ has a wide orbital gap, 4.27 eV, and almost zero electron affinity. It indicates that $C_{24}H_{12}N_{12}$ has high electronic stability.

Due to higher electron affinity and ionization potential for $C_{4n}H_{2n}N_{2n}$ ($n = 3$, 4) species, it is more difficult for them to lose an electron but easier to accept one. However, the $C_{4n}H_{2n}N_{2n}$ ($n = 5-8$) species have higher ionization potential and lower electron affinity, and it is thus more difficult for them to lose an electron than to accept one. So $C_{28}H_{14}N_{14}$ and $C_{32}H_{16}N_{16}$ cages have also higher electronic stability.

3.4. Aromatic Character. As well-known, electron delocalization may lead to conjugation interaction and enhancement of thermal stabilities accordingly. Aromatic character is an important index to characterize the electron delocalization. The aromaticity at a specified position can be evaluated by the NICS value using a ghost atom placed in this position. To study the position dependence of NICS, nineteen representative points along the D_n ($n = 3-8$) axis of $C_{4n}H_{2n}N_{2n}$ ($n = 3-8$) molecules at equal intervals are taken for our NICS calculation, with three of them at the geometric center, the ring center of top polygon, and the ring center of bottom polygon for each molecule. Eight points of them are specified outside the cages and the remaining inside. All calculated NICS results were plotted in Figure 6, and those points on the top, center, and bottom polygons were also labeled for clarity.

The negative NICS value at a specified position means high electron density, and thus a strong shielding effect exists thereabout. In all positions above the top polygon and below the bottom polygon, the absolute value of negative NICS decreases gradually. For those points inside the cage, only two compounds show negative NICS, while the others are all positive, namely, $C_{20}H_{10}N_{10}$ has a slightly small negative NICS values and $C_{24}H_{12}N_{12}$ has a medium negative values. The existence of ring current in $C_{20}H_{10}N_{10}$ and $C_{24}H_{12}N_{12}$ cages indicates their aromaticity. It supports the fact that they have relatively higher chemical stability among $C_{4n}H_{2n}N_{2n}$ ($n = 3-8$) series based on the evaluation of group ε_0 and group heat of formation.

The deshielding effect along the axis inside the cage are strong in $C_{12}H_6N_6$ and $C_{16}H_8N_8$, that in $C_{28}H_{14}N_{14}$ is quite small, and that in $C_{32}H_{16}N_{16}$ is intermediate. It is shown in Figure 6 that the distribution of NICS along the axis looks like cones for $C_{12}H_6N_6$ and $C_{16}H_8N_8$, a thin columnar shape for $C_{28}H_{14}N_{14}$, and a spindly cone for $C_{32}H_{16}N_{16}$ inside these cages. Figure 6 also shows weak aromaticity above the top and below the bottom polygons for the molecules with seven- and eight-membered rings, while those points inside the two polygons show obvious weak antiaromaticity.

It is worthy to note that all the calculated NICS values in $C_{4n}H_{2n}N_{2n}$ ($n = 3-8$) cages herein are very different from those in $C_{4n}N_{2n}$ ($n = 3-8$) species.[12] For example, the NICS values in $C_{4n}N_{2n}$ ($n = 6$) show positive NICS population along C_6 axis and the other show negative NICS population along the C_n axis inside the cage. The difference between the >N—N< bonds matrix in the $C_{4n}N_{2n}$ ($n = 3-8$) species and the >C═C< bonds matrix in the $C_{4n}H_{2n}N_{2n}$ ($n = 3-8$) explains their respective special aromaticity.

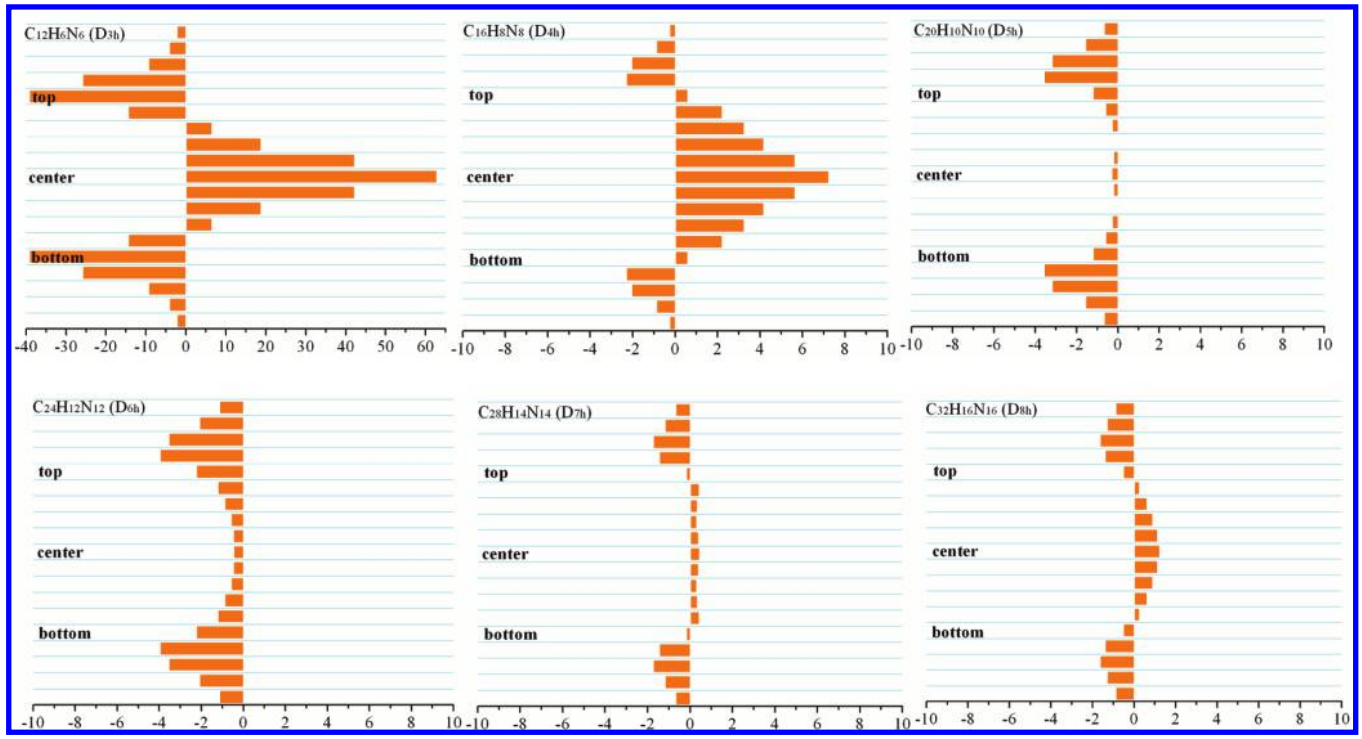

Figure 6. NICS (ppm) values of title compounds.

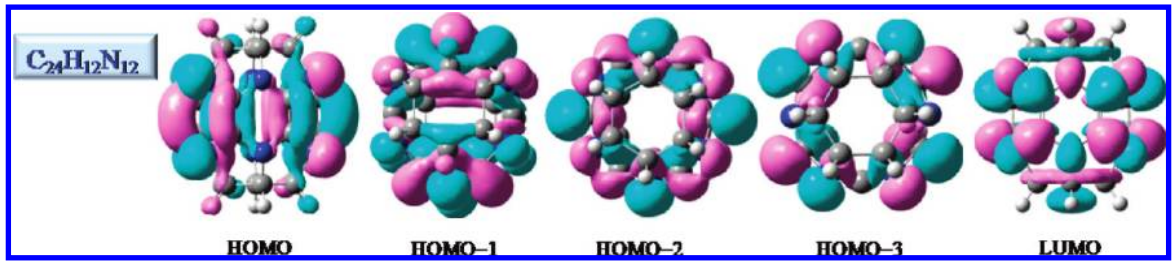

Figure 7. Molecular orbitals in $C_{24}H_{12}N_{12}$ (D_{6h}).

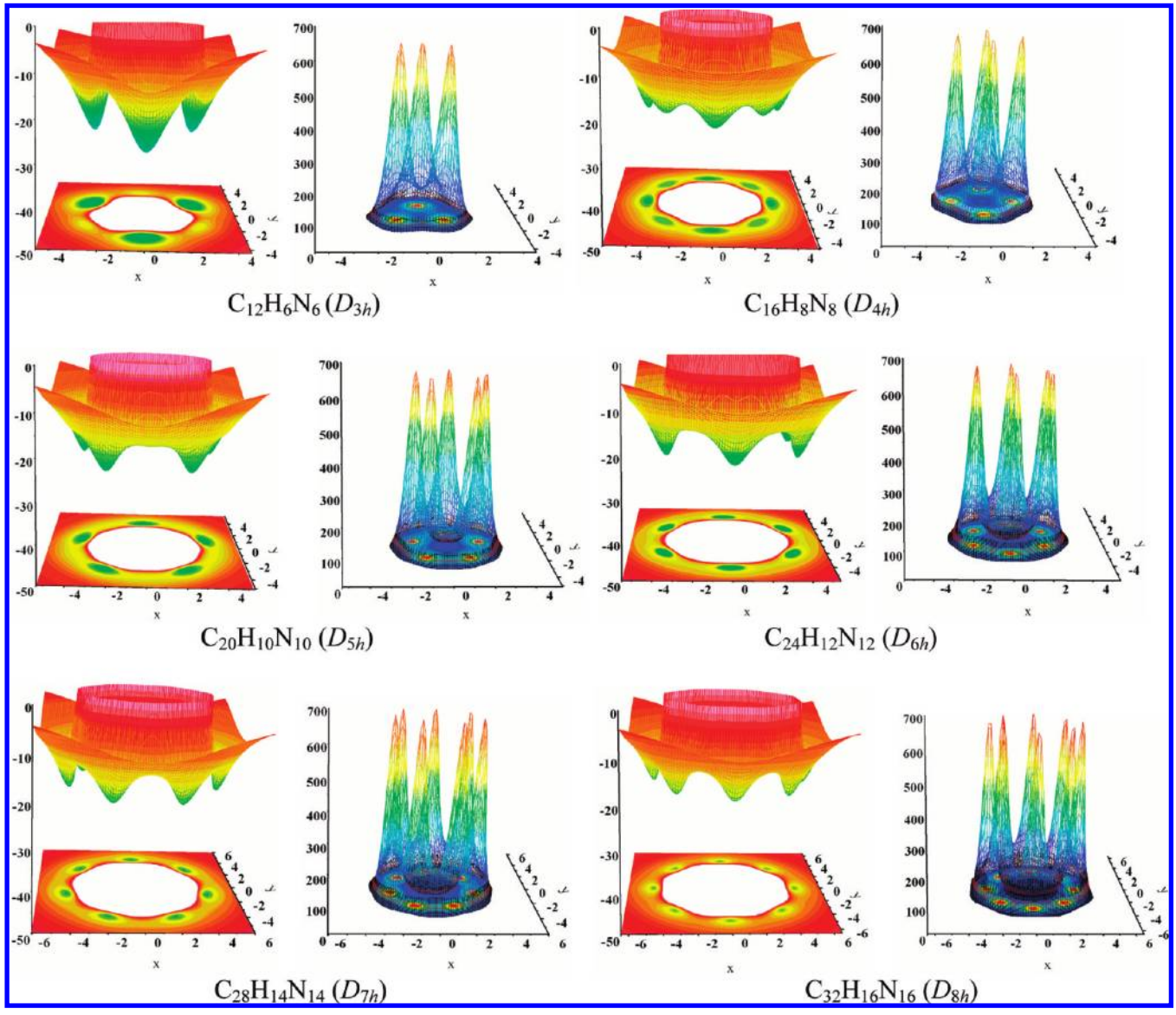

Figure 8. Contour maps of electrostatic potential projected on the molecular *XY* plane, i.e., σ_h symmetry plane. Negative values in left and positive in right for each molecule; the unit is kcal/mol.

The abnormal bond length of the C−C bond (1.517 Å) on the top and bottom polygons of $C_{12}H_6N_6$ can be explained by the very negative NICS values at the top and bottom triangles. The strong σ-conjugative effect[20] is responsible for the short C−C bond length therein. The positions along the D_{3h} axis inside the cage of $C_{12}H_6N_6$ show very large positive NICS values. The three >C═C< bonds parallel to the axis might be attributed to this phenomenon. Nevertheless, all positions between the top and bottom polygons in $C_{16}H_8N_8$ show positive NICS values. It is explained that the antiaromatic character from cyclobutane cycles on the top and bottom polygons contributes a small positive NICS values as in the case of cyclobutane in cubane.[21] NICS values in center region of $C_{16}H_8N_8$ show intermediate positive NICS caused by the four >C═C< bonds.

Although all those points distributing outside of the cages show negative NICS values, $C_{12}H_6N_6$ gives the most negative one. It is indicated that a strong shielding effect exists on the top and bottom triangles and their vicinity. A bigger ^{1}H NMR shielding constant in $C_{12}H_6N_6$, 29.12 ppm, was calculated at the B3LYP/cc-pVDZ level. In comparison, those shielding constants of hydrogen in $C_{4n}H_{2n}N_{2n}$ (n = 4−8) cages, 27.59, 27.08, 27.41, 27.16, and 27.05 ppm, were obtained at the same theoretical level. A stronger paramagnetic deshielding effect exists for peripheral hydrogens in $C_{12}H_6N_6$. It is similar to the

case of cycloalkanes C_nH_{2n} ($n = 3-8$) about the magnitude order of ^1H NMR shielding constants, and other result.[22]

To better comprehend the good stability and aromatic character of $C_{24}H_{12}N_{12}$, its molecular orbitals are plotted in Figure 7. Although no significant Π-conjugation is found, there is a moderate lateral delocalization effect. The degenerate HOMO and HOMO−1 orbitals contribute mainly to the lateral delocalization effect so as to give slight negative NICS values along the central part of the axis.

3.5. Electrostatic Potential. Electrostatic potential (ESP) calculations can be used to estimate the chemical behavior of molecules. A quick look at the ESP plots depicted in Figure 8, the projection plots on XY plane perpendicular to D_n axis, the ESP inside the cages has positive values, and that outside the cages has negative values. A minimum value of −29.19 kcal/mol is found for $C_{12}N_6H_6$, and −24.02, −25.33, −24.11, −22.42, and −20.75 kcal/mol are for $C_{4n}H_{2n}N_{2n}$ ($n = 4-8$), respectively. Those regions with negative values are all located outside the cage. The regions with more negative values lie at the center of pyrazine groups. So these regions are attractive to cation species and electrophilic reagents.

Although delocalization ring current was found in $C_{24}H_{12}N_{12}$ by NICS calculation, the ESP values inside the cage are still positive because of the ESP dependence on both the electrons and nuclei.

The other title molecules also show the same behavior. Although the ESP values in other planes parallel to the σ_h symmetry plane are not given, they have also the same sign, i.e., positive inside the cage and negative outside. The bending of a planar Π-conjugate system squeezes its wave function out of the cage due to the electron−electron repulsion. Electrons are predicted to easily penetrate through these cages. Some new special properties are expected. Due to scarcely any positive ESPs localized over covalent bonds, it is believed that they have relatively insensitive character based on the qualitative rule of explosive sensitivity of Rice's criterion.[23] Therefore, in consideration of those results mentioned above, $C_{24}H_{12}N_{12}$ and its substituted products (e.g., substituted by F, CN, etc.) deserve to be studied further.

4. Conclusions

$C_{4n}H_{2n}N_{2n}$ ($n = 3-8$) cages with D_{nh} symmetry were investigated by DFT theory. Their nitrated products were also designed selectively and optimized. Our study focused on the relationship between molecular structures and relative stabilities. Important conclusions are drawn as follows:

The $C_{4n}H_{2n}N_{2n}$ ($n = 3-8$) series exhibit an obvious caging effect. The distances $d_{C=C}$ and d_{plane} decrease from $n = 3$ to 8 monotonously. The C−C bond lengths on the top and bottom polygongs increase from $n = 4$ to 8 except the abnormality in $C_{12}H_6N_6$. For $C_{4n}N_{4n}O_{4n}$ ($n = 4, 5$) and $C_{4n}H_nN_{3n}O_{2n}$ ($n = 4, 6, 8$) series, $d_{C=C}$ becomes shorter or the C=C bonds become stronger as n increases. $C_{12}N_{12}O_{12}$ is the exception and is predicted to be less stable. The average d_{C-C} in $C_{4n}N_{4n}O_{4n}$ ($n = 3, 4, 5$) is longer and that in $C_{4n}H_nN_{3n}O_{2n}$ ($n = 4, 6, 8$) is shorter in comparison to that in their precursor before nitration. It is explained that more nitration causes more repulsive force to decrease their stability.

Among $C_{4n}H_{2n}N_{2n}$ ($n = 3-8$), $C_{24}H_{12}N_{12}$ is the most stable molecule by the calculation of group energy and group heat of formation. The same approach predicted that the nitration product of $C_{20}H_{10}N_{10}$ among $C_{4n}N_{4n}O_{4n}$ ($n = 3, 4, 5$) and that of $C_{24}H_{12}N_{12}$ among $C_{4n}H_nN_{3n}O_{2n}$ ($n = 4, 6, 8$) are the most stable molecules. The investigation of orbital properties supports the electronic stability of $C_{24}H_{12}N_{12}$. The half nitration product of $C_{24}H_{12}N_{12}$ is desirable as a promising candidate of high energy matter.

The NICS analysis provides an insight about molecular aromatic character and thus the relative stability of $C_{20}H_{10}N_{10}$ and $C_{24}H_{12}N_{12}$, which were consistent with the results of thermochemical calculation. It is considered that the pyrazine fragments in the title compounds play an important role on the formation of their aromaticity.

Electrostatic potential calculation predicts them to be insensitive. It is predicted elections can easily penetrate through these cages. So the $C_{24}H_{12}N_{12}$ molecule with relative high stability could show some special properties and is expected to be synthesized.

Supporting Information Available: Geometrical parameters, Hirshfeld charges, the change of reaction enthalpy of isodesmic reactions, isodesmic reaction equations, and orbital energetic values. This material is available free of charge via the Internet at http://pubs.acs.org.

References and Notes

(1) Okamoto, Y. *J. Phys. Chem. A* **2001**, *105*, 7634.
(2) Paulus, B. *Phys. Chem. Chem. Phys.* **2003**, *5*, 3364.
(3) Malolepsza, E.; Witek, H. A.; Irle, S. *J. Phys. Chem. A* **2007**, *111*, 6649.
(4) Ternansky, R. J.; Balogh, D. W.; Paquette, L. A. *J. Am. Chem. Soc.* **1982**, *104*, 4503.
(5) Disch, R. L.; Schulman, J. M. *J. Am. Chem. Soc.* **1988**, *110*, 2102.
(6) King, R. B. *Chem. Rev.* **2001**, *101*, 1119.
(7) Chen, Z.; Jiao, H.; Hirsch, A.; Thiel, W. *Chem. Phys. Lett.* **2000**, *329*, 47.
(8) Jursic, B. S. *J. Mol. Struct. (THEOCHEM)* **2000**, *530*, 21.
(9) Wang, L. J.; Zgierski, M. Z.; Mezey, P. G. *J. Phys. Chem. A* **2003**, *107*, 2080.
(10) Bruney, L. Y.; Strout, D. L. *J. Phys. Chem. A* **2003**, *107*, 5840.
(11) Strout, D. L. *J. Phys. Chem. A* **2003**, *107*, 1647.
(12) Shi, L.-W.; Chen, B.; Zhou, J.-H.; Zhang, T.; Kang, Q.; Chen, M.-B. *J. Phys. Chem. A* **2008**, *112*, 11724.
(13) Chernichenko, K. Y.; Sumerin, V. V.; Shpanchenko, R. V.; Balenkova, E. S.; Nenajdenko, V. G. *Angew. Chem., Int. Ed.* **2006**, *45*, 7367.
(14) Strout, D. L. *J. Chem. Theory Comput.* **2005**, *1*, 561.
(15) Choi, J.; Harcup, J.; Yee, A. F.; Zhu, Q.; Laine, R. M. *J. Am. Chem. Soc.* **2001**, *123*, 11420.
(16) Woon, D. E.; Dunning, T. H., Jr. *J. Chem. Phys.* **1993**, *98*, 1358.
(17) (a) Schleye, P. v. R.; Maerker, C.; Dransfeld, A.; Jiao, H.; van Eikema Hommes, N. J. R. *J. Am. Chem. Soc.* **1996**, *118*, 6317. (b) Chen, Z.; Wannere, C. S.; Corminboeuf, C.; Puchta, R.; Schleyer, P. v. R. *Chem. Rev.* **2005**, *105*, 3842.
(18) Wolinski, K.; Hilton, J. F.; Pulay, P. *J. Am. Chem. Soc.* **1990**, *112*, 8251.
(19) (a) Balanarayan, P.; Gadre, S. R. *J. Chem. Phys.* **2006**, *124*, 204113. (b) Balanarayan, P.; Gadre, S. R. *J. Am. Chem. Soc.* **2006**, *128*, 10702.
(20) Fowler, P. W.; Baker, J.; Lillington, M. *Theor. Chem. Acc.* **2007**, *118*, 123.
(21) Moran, D.; Manoharan, M.; Heine, T.; Schleyer, P. v. R. *Org. Lett.* **2003**, *5*, 23.
(22) Pelloni, S.; Lazzeretti, P.; Zanasi, R. *J. Phys. Chem. A* **2007**, *111*, 8163.
(23) Rice, B. M.; Hare, J. J. *J. Phys. Chem. A* **2002**, *106*, 1770.

JP911788P